WIRELESS COMMUNICATIONS AND MOBILE COMPUTING
*Wirel. Commun. Mob. Comput.* 2014; **14**:339–354
Published online 16 January 2012 in Wiley Online Library (wileyonlinelibrary.com). DOI: 10.1002/wcm.1252

RESEARCH ARTICLE

# IEEE 802.11 medium access control enhancements based on simultaneous multiple-input multiple-output bandwidth sharing

Abduladhim Ashtaiwi[1], Ahmed Iyanda Sulyman[2] and Hossam S. Hassanein[2,3]*

[1] Department of Electrical and Computer Engineering, Queen's University, Kingston, ON, Canada
[2] Electrical Engineering Department, King Saud University, Riyadh, Saudi Arabia
[3] School of Computing, Queen's University, Kingston, ON, Canada

## ABSTRACT

The demand for higher data rate has spurred the adoption of multiple-input multiple-output (MIMO) transmission techniques in IEEE 802.11 products. MIMO techniques provide an additional spatial dimension that can significantly increase the channel capacity. A number of multiuser MIMO system have been proposed, where the multiple antenna at the physical layer are employed for multiuser access, allowing multiple users to share the same bandwidth. As these MIMO physical layer technologies further evolve, the usable bandwidth per application increases; hence, the average service time per application decreases. However, in the IEEE 802.11 distributed coordination function-based systems, a considerable amount of bandwidth is wasted during the medium access and coordination process. Therefore, as the usable bandwidth is enhanced using MIMO technology, the bandwidth wastage of medium access and coordination becomes a significant performance bottleneck. Hence, there is a fundamental need for bandwidth sharing schemes at the medium access control (MAC) layer where multiple connections can concurrently use the increased bandwidth provided by the physical layer MIMO technologies. In this paper, we propose the MIMO-aware rate splitting (MRS) MAC protocol and examine its behavior under different scenarios. MRS is a distributed MAC protocol where nodes locally cooperate with one another to share bandwidth via splitting the spatial channels of MIMO systems. Simulation results of MRS protocol are obtained and compared with those of IEEE 802.11n protocol. We show that our proposed MRS scheme can significantly outperform the IEEE 802.11n in medium access delay and throughput. Copyright © 2012 John Wiley & Sons, Ltd.

**KEYWORDS**
wireless LAN (WLAN); medium access control (MAC); scheduling; MIMO-aware MAC protocol

***Correspondence**
Hossam S. Hassanein, School of Computing, Queen's University, Kingston, ON, Canada.
E-mail: hossam@cs.queensu.ca

## 1. INTRODUCTION

Wireless local area networks (WLANs) have gained popularity at an unprecedented rate. They are widely used at home, at work, and in public hot spot locations. To enhance data rate of WLAN, the IEEE standardization committee formed the 802.11 Task Group "N" to develop the IEEE 802.11n amendment, which exploits the MIMO physical layer technique for data rate enhancements. Under suitable channel fading conditions, MIMO transmission provide an additional spatial dimension (or degree of freedom) that can be exploited for higher data rate by spatially multiplexing several data streams onto the MIMO channel, yielding an increase in the WLAN channel capacity (beyond 100 Mbps) [1,2]. MIMO channel capacity is expected to further increase as multiuser MIMO-beamforming (MIMO-BF) techniques at the physical layer become mature. Multiuser MIMO-BF systems allow two or more users with MIMO devices share a single physical layer channel for their data transmissions, taking advantage of the users' different spatial locations. This paper focuses on the MAC layer data rate enhancement that takes advantage of these physical layer MIMO techniques. The IEEE 802.11 distributed coordination function (DCF) is the legacy MAC layer protocol for the Wi-Fi systems. However, in the IEEE 802.11 DCF-based systems, switching to the next pending connection requires a considerable amount of time wasted in the medium access and coordination mechanisms. As the usable bandwidth per application increases using MIMO technologies, the wasted bandwidth in the medium access and coordination becomes noticeable and turns to be a performance bottleneck. To efficiently utilize the bandwidth enhancements in such decentralized systems, there is a fundamental need for medium access control (MAC) protocols, which allow multiple connections to concurrently share the enhanced bandwidth provided via MIMO transmissions.

There have been few attempts in the literature to develop MIMO-aware MAC protocols. The work in [3] proposes a rate scheduling scheme based on stream control medium access by sensing over two hops using request-to-send (RTS) and clear-to-send (CTS) frame exchanges. The scheme enables light-loaded connections to concurrently share the available rate while it schedules overloaded ones to use the full rate. The work in [4] proposes a MAC protocol that employs spatial multiplexing. A major assumption in [4] is that the nodes in the network are synchronized and that the connections evenly share the antennas without prior channel quality assessment. In [5], the authors proposed a MIMO-aware MAC protocol that allows the integration of MIMO into the IEEE 802.11 WLAN by extending the control frames, RTS, CTS, and acknowledgement(ACK), to M-RTS, M-CTS, and M-ACK, respectively. The extended frames were then used for performing negotiation about the active antenna elements, channel estimation, and the selection of MIMO encoding techniques. Multiple access using MIMO spatial channels, as presented in this work, were, however, not considered. In [6], the authors considered the encoding–decoding delay incurred by MIMO systems. To reduce the coding delay, the authors skipped the use of the control packets, RTS, CTS, and ACK, by allowing direct data transmission on the medium. In [7], the authors proposed a scheme that involves transmit antenna and data rate selection based on an optimal trade-off between MIMO spatial multiplexing and MIMO diversity/coding technique, based on the channel state information (CSI). The work in [8], [9], and [10] introduce MAC protocols based on MIMO-BF to create a pattern of constructive and destructive interference to selectively listen or ignore a particular user transmissions. However, the main issue with these schemes is that inaccuracies in CSI can result in collision or interference to unintended users.

To boost the system usability and to efficiently utilize the enhanced bandwidth provided by MIMO systems without the risk of collisions, we introduce in this work a novel MIMO-aware rate splitting (MRS) MAC protocol. Rather than relying on interference canceling via MIMO-BF, the proposed MRS system relies on a novel MIMO spatial channel splitting for its bandwidth enhancement. MRS allows connections to concurrently share the enhanced bandwidth via carefully designed MIMO spatial channel-based rate splitting. The MRS protocol is a distributed MAC protocol that enables nodes to locally cooperate with other nodes in their vicinities to first estimate the spatial channels' status, then to translate the required data rate into a number denoting spatial channel requirements, and finally to reserve the required spatial channels avoiding any collision. The proposed MRS protocol opens up some new research directions for many bandwidth management schemes in WLANs and ad hoc networks. In [11], initial results on the spatial channels sharing concept in wireless mesh networks links were reported for concurrently meeting different data rate demand of different connections. Unlike in [11], however, in this work, we broadly expose the spatial channels sharing concept to a wider network characteristics, and we also highlight the potential capabilities of the proposed algorithm to improve the overall system usability. The performance of the MRS is evaluated using OPNET (OPNET Technologies, Inc., Bethesda, MD, USA) interfaced with MATLAB (The MathWorks Inc., Natick, MA, USA) for various scenarios for different values of requested rates, interference zones, and different communication environments. We show that our proposed MRS scheme significantly outperforms the IEEE 802.11n standard MAC protocol.

The remainder of this paper is organized as follows. Section 2 details the MIMO channel estimation and interference model assumed in this work. The MRS MAC protocol is discussed in details in Section 3. Section 4 presents some properties of the MRS scheme. Performance evaluation is presented in Section 5. Finally, concluding remarks are presented in Section 6.

## 2. MULTIPLE-INPUT MULTIPLE-OUTPUT CHANNEL ESTIMATION AND INTERFERENCE MODEL IN WIRELESS LOCAL AREA NETWORKS

The IEEE 802.11 Task Group "N" (IEEE 802.11n) [12] builds on the legacy IEEE 802.11 standard by adding multiple transmit and receive antennas, each with an RF chain that is capable of simultaneous receiving or transmitting traffic. To help receivers estimate the spatial channel status and recover the transmitted signals, the IEEE 802.11n amendment [12] recommends transmitting a known communication setup frame, called sounding frames (SFs), through all transmit antennas. As defined in the IEEE 802.11n amendment, the SFs can either be attached to the MAC protocol data unit frames if no channel feedback information is required at the transmitter node or be sent through two-way handshake exchanges. In the latter case, the transmitter sends a channel sounding request (CSQ), and the receiver responds with a channels sounding response (CSR). The CSQ and CSR exchange is performed if the channel feedback information is required at both sides, that is, the transmitter and the receiver nodes. During the CSQ period, the transmitter node concurrently sends one SF through each transmit antenna element. Then the receiver, after receiving the CSQ frames, responds by concurrently sending one SF through each transmit antenna element of the receiver node, where the latter is performed during CSR period. In this work, we consider two-way handshake exchanges of the CSQ and CSR for estimating the MIMO channels.

For the MIMO interference models in WLANs, we consider MIMO links in ad hoc networks with $n$ stationary nodes. In this type of network, there is no central control for data transmissions, and all nodes have similar characteristics. Hence, we do not distinguish between uplink and downlink channels. As shown in Figure 1, the network model has $k$ connection pairs, where $v_i, \{i = 1, 2, \ldots, k\}$ denote the $i$th connection pair. For simplicity, each connection pair has one node as a transmitter ($v_i^{\mathrm{tx}}$) and another node as a receiver ($v_i^{\mathrm{rx}}$) all the time. All nodes are equipped with $n_{\mathrm{t}}$ transmit and $n_{\mathrm{r}}$ receive antennas. The $v_{i\mathrm{th}}^{\mathrm{rx}}$ receiver node receives a desired message from a desired transmitter belonging to the same connection pair and $\Gamma$ interfering messages from nearby active connections. $\Gamma$ is any subset of $k-1$ connections that may concurrently communicate with their connection pairs during the same time in which this connection is active.

The received signal $Y_i$ at the $v_{i\mathrm{th}}^{\mathrm{rx}}$ receive node is modeled as

$$Y_{v_{i\mathrm{th}}^{\mathrm{rx}}} = P_{\mathrm{d}} H_{\mathrm{d}} + \sum_{i \in \Gamma} H_I^i P_I^i + n_s \tag{1}$$

where $Y_{v_{i\mathrm{th}}^{\mathrm{rx}}}$ is the $(n_r \times 1)$ received signal vector, $P_{\mathrm{d}}$ is the total transmit power of desired transmitter node, $P_I^i$ is the total transmit power of the $v_{i\mathrm{th}}^{\mathrm{tx}}$ interfering node [1]. $H_{\mathrm{d}}$ is the $(n_{\mathrm{r}} \times \tilde{n}_{\mathrm{t}})$ channel fading coefficient matrix between the $v_{i\mathrm{th}}^{\mathrm{rx}}$ receiver and its corresponding transmitter $v_{i\mathrm{th}}^{\mathrm{tx}}$. $\tilde{n}_{\mathrm{t}}$ denotes the number of active antennas during the transmission, where $\tilde{n}_{\mathrm{t}} \le n_{\mathrm{t}}$. $H_{\mathrm{d}}$ is expressed as

$$H_{\mathrm{d}} = \begin{bmatrix} h_{\mathrm{d}}(1,1) & \ldots & h_{\mathrm{d}}(1,\tilde{n}_{\mathrm{t}}) \\ \vdots & \ddots & \vdots \\ h_{\mathrm{d}}(n_{\mathrm{r}},1) & \ldots & h_{\mathrm{d}}(n_{\mathrm{r}},\tilde{n}_{\mathrm{t}}) \end{bmatrix} \tag{2}$$

where $h_{\mathrm{d}}(i,j)$ is the channel fading coefficient between the $j$th transmit antenna to the $i$th receive antenna for the desired connection and is modeled as $h_{\mathrm{d}}(i,j) = (\lambda/4\pi D)^{\eta} + \chi_{\sigma}$, where $\lambda$ is the wavelength, $D$ is the distance between the $v_{i\mathrm{th}}^{\mathrm{tx}}$ transmitter and its intended receiver, $\eta$ is the path loss exponent, and $\chi_{\sigma}$ is the shadow fading effect and is modeled as zero-mean, Gaussian random variable, with standard deviation, $\sigma$ (dB), added to the path loss. $H_I^i$ in Equation (1) is the channel fading coefficient matrix between the $i$th interfering connection and the $v_{i\mathrm{th}}^{\mathrm{rx}}$ receiver. $H_I^i$ is expressed as

$$H_I^i = \begin{bmatrix} h_I(1,1) & \ldots & h_I(i,\tilde{n}_{\mathrm{t}}) \\ \vdots & \ddots & \vdots \\ h_I(n_{\mathrm{r}},1) & \ldots & h_I(n_{\mathrm{r}},\tilde{n}_{\mathrm{t}}) \end{bmatrix}, \; i = 1, 2, \ldots, \Gamma \tag{3}$$

where $h_I(i,j)$ is the channel fading coefficient between the $j$th transmit antenna element of the interfering connection and the $i$th receive antenna element of the receiving node. $h_I(i,j)$ is modeled the same way as $h_{\mathrm{d}}(i,j)$ except that $R$, the distance between the $v_{i\mathrm{th}}$ interfering connection and the receiver node, is used instead of $D$ to compute the path loss. $n_s$ in Equation (1) denotes the additive noise signal, modeled as complex Gaussian random variable with a zero mean and a variance of 1. We consider a Rayleigh slow fading channel in a very rich scattering environment and that the transmit and receiver antennas are spaced sufficiently apart such that the channel gain matrix $H_{\mathrm{d}}$ and $H_I^i$ are independently identically distributed. We also consider that the spatial degree of freedom ($\varphi$) is equal to $\min(n_{\mathrm{r}}, n_{\mathrm{t}})$ [13,14]. For simplicity, we assume that the same power is allocated to each and every transmit antenna element and is equal to the total transmit power constraint divided by the number of antennas $n_{\mathrm{t}}$. We assume that during the reception period, nodes always activate all the available receive antennas and that they only activate the required transmit antenna elements during the transmission period on the basis of their rate requirements.

Let horzcat[ ]† represent the horizontal concatenation of multiple matrices. Let $H_{\mathrm{cat}}$ denote the concatenated matrix of all interfering matrices that are currently interfering with this connection pair at the same time, $H_{\mathrm{cat}} = \mathrm{horzcat}[H_I^1, H_I^2, \ldots, H_I^{\Gamma}]$.

We denote the maximum error-free rate that the channel can support by $C_{\mathrm{T}}$. If $C_{\mathrm{T}}$ is to be used by $k$ connection pairs, the sum of the partially used capacities by all connections must satisfy

$$\sum_{i=1}^{k} C_i \le C_{\mathrm{T}} \tag{4}$$

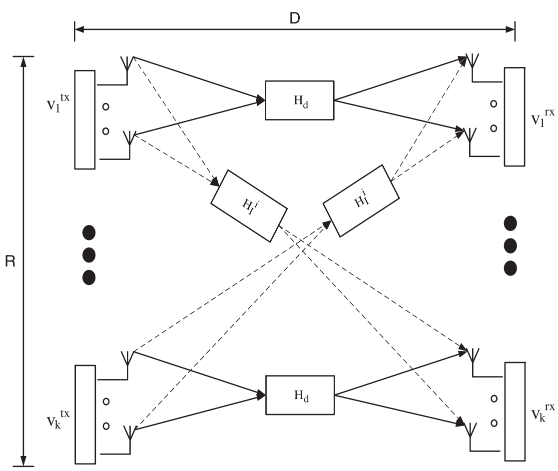


**Figure 1.** Interference channel model.

†Similar to the MATLAB notations, $\mathrm{horzcat}[H_I^1, H_I^2, \ldots, H_I^{\Gamma}]$ is used to horizontally concatenate matrices. We also use $H_{\mathrm{cat}}(:, H_I^i)$ to denote the removal of the matrix $H_I^i$ from the matrix $H_{\mathrm{cat}}$ [15].

where $C_i$ is the partial bandwidth used by the $v_{i\text{th}}$ connection and is given by

$$C_i = \sum_{j=1}^{\tilde{n}_t} \log_2 \Big(1 + P_i h_j^H \times \Big(I_{n_r} + \text{horzcat}\Big[P_i \tilde{H}_j \tilde{H}_j^H,\ P_I H_{\text{cat}} H_{\text{cat}}^H\Big]\Big)^{-1} h_j\Big) \quad (5)$$

$h_j^H$ is the transpose of the $j$th column of the $H_d$ matrix, and $\tilde{H}_j$ is the remaining matrix after removing the $j$th column from $H_d$.

## 3. MULTIPLE INPUT MULTIPLE OUTPUT-AWARE RATE SPLITTING

The MRS is a MAC protocol that allows multiple concurrent communications by enabling spatial channel splitting of MIMO transmission links. The MRS scheme implements this by first estimating the spatial channel requirements of each connection. This is achieved by translating the requested data rate of each connection into a number of spatial channel requirements. Then the MRS scheme broadcasts the required spatial channels using the RTS–CTS frame exchange and, finally, use the reserved spatial channels for data communications. The following phases cover the functional aspects of the MRS cheme.

(1) Medium contention phase: the MIMO-based medium access procedure with which active nodes either start or suspend medium contention.
(2) Channel sounding phase (CSP): an exchange of small physical layer frames called SFs to induce the CSI from the transmitter to the receiver and vice versa.
(3) Slot scheduling and broadcasting phase (SSBP): Using the CSI, the accessing connection pair first translates the connection's required data rate into a number of antenna requirements, finds next a slot (time interval) at which these requested antennas are available, and broadcasts the desired slot reservation attributes (RAs) using RTS–CTS packet exchange. The slot's RA is described by four parameters: the slot starting time ($\tilde{\epsilon}_s$), ending time ($\tilde{\epsilon}_e$), tolerated interference ($\tilde{I}_t$), and the number of antennas intended to be used ($\tilde{n}_t$).
(4) Communication phase (CP): the reserved slot period during which the connection pair starts data and ACK packet exchange.

Figure 2 depicts the MRS MAC protocol phases. In this figure, we illustrate the frame exchange order, such as the transmission order of the sounding, RTS, CTS, Data, and ACK frames. We also illustrate the contention areas by indicating whether nodes are in the same or different contention areas. For example, nodes 1 and 3 are in one contention area, whereas nodes 2, 4, and 6 are in another contention area. Furthermore, we illustrate in the figure the spatial streams used by each connection, $U_a^i$, by indicating how many antennas a connection pair is currently using. For example $U_a = 4$ for the connection pair (1–2), whereas $U_a = 2$ for the connection pairs (3–4) and (5–6). Finally, we illustrate in the figure, the medium contention procedure using the DCF interframe space (IFS), or DIFS,

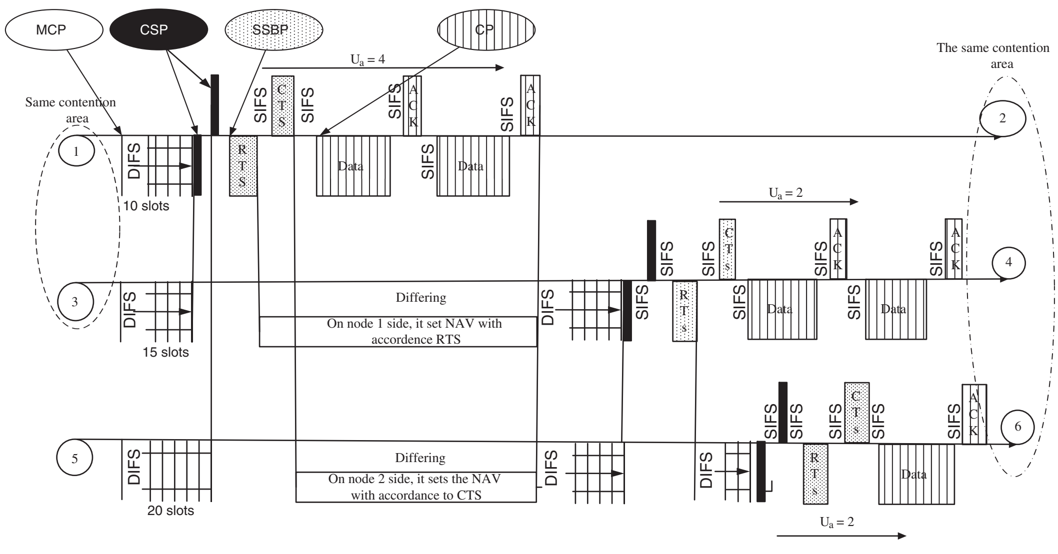


**Figure 2.** The multiple input multiple output-aware rate splitting protocol main phases, deferral, and concurrent transmissions. MCP, medium contention phase; CSP, channel sounding phase; SSBP, slot scheduling and broadcasting phase; CP, communication phase; DIFS, distributed coordination function interframe space; SIFS, short interframe space; RTS, ready to send; CTS, clear to send; ACK, acknowledgement; NAV, network allocation vector.


Wirel. Commun. Mob. Comput. 2014; 14:339–354 © 2012 John Wiley & Sons, Ltd.
DOI: 10.1002/wcm

and the countdown process. For the countdown process, we detailed the numbers of backoff slots of each connection pair (e.g., 10 slots for the connection pair (1–2), 15 slots for the connection pair (3–4), and 20 slots for the connection pair (5–6)), how backoff slots are decremented, and which node reaches zero first and consequently gaining access to the medium. Notice also from this figure that the case $U_a = 4$ depicts the scenario whereby the connection pair (1–2) uses all the available MIMO spatial channels, whereas the case $U_a = 2$ depicts the scenario whereby two connection pairs, (3–4) and (5–6), share the available MIMO spatial channels to utilize their reserved slot periods.

Medium contention phase starts when a node has data and is ready for transmission. A node monitors the medium activity until an idle period, equal to DIFS, has been observed. Unlike the IEEE 802.11 MAC protocol, the idle and busy medium status are defined on the basis of the spatial channels control multiple access mechanism. In this mechanism, spatial channel availability is observed physically through the air interface, by detecting the current usable spatial channel(s), as well as virtually. The virtual carrier sensing is performed by having the $i$th connection pair broadcast the intended spatial channel(s) to be used ($U_a^i$) and by storing this information in the network allocation vector (NAV) table whenever nodes overhear RTS and CTS. Hence, the NAV keeps track of the remaining and the reserved spatial streams. On the basis of the total currently used spatial channel(s), $U_t = \sum_{i=1}^{\Gamma+1} U_a^i$, the instantaneous medium status is represented as

$$\text{Medium status} = \begin{cases} \text{Idle} & \text{if } U_t < \varphi \\ \text{Busy} & \text{if } U_t = \varphi \\ \text{Collision} & \text{if } U_t > \varphi \end{cases} \quad (6)$$

In case the medium is sensed busy ($U_t \geq \varphi$), a BF is consequently selected from a defined contention window (CW) range, that is, BF = uniform$(0, CW)$, where $CW_{\min} < CW < CW_{\max}$. The backoff counter is decremented by 1 only when the $U_t < \varphi$ and is frozen when the $U_t \geq \varphi$. Once the backoff timer counter reaches 0, the node is authorized to start SFs exchange.

The CSP is the phase during which connection pairs start their SF exchanges (i.e., the CSQ and CSR exchange). The CSP phase starts when the connection pair transmitter sends a CSQ sequence and ends when the connection pair receiver responds with CSR sequence. In both cases, the $n_t$ SFs are transmitted from each node over the available $n_t$ antennas. At the end of the CSP phase, both the transmitter and the receiver of the $i$th connection obtain the CSI of the channel between them. Nodes around the $i$th connection pair can use the received SFs to assess the channel status between them and the transmitter/receiver or both. This information is continuously stored per node in the NAV table and updated whenever a new transmission is heard for the same $i$th connection pairs.

Figure 3 shows how a connection pair, say, (3–4), can reserve a future slot, that is, a slot to be used for data transmission between nodes 3 and 4, after $\Delta$ time interval from the reservation time. This happens when nodes could not find suitable slots for the desired bandwidth immediately. Figure 3 also shows how connection pair (5–6) starts a medium access contention and reserves the remaining available bandwidth (two spatial channels) from the end of SSBP to the start of the CP of connection pair (3–4).

Figure 4 shows that nodes located in different contention areas may cause slot mismatch, that is, the desired slot on the transmitter side has different RAs from that of the receiver side. The MRS MAC scheme addresses the slot mismatch problem by mandating nodes to send one

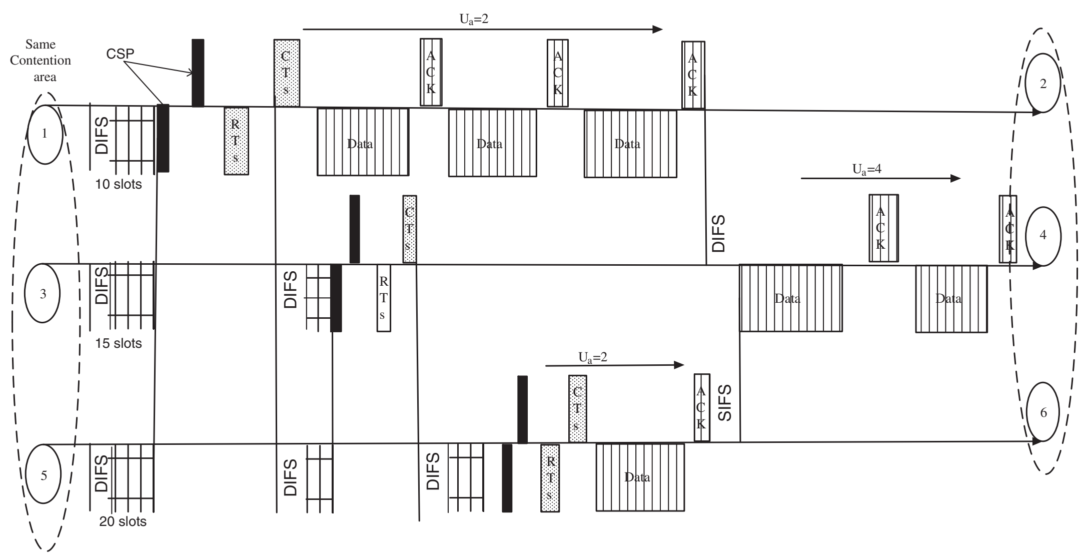


**Figure 3.** Reserving an immediate and delayed slots. CSP, channel sounding phase; DIFS, distributed coordination function interframe space; SIFS, short interframe space; RTS, ready to send; CTS, clear to send; ACK, acknowledgement.


DOI: 10.1002/wcm

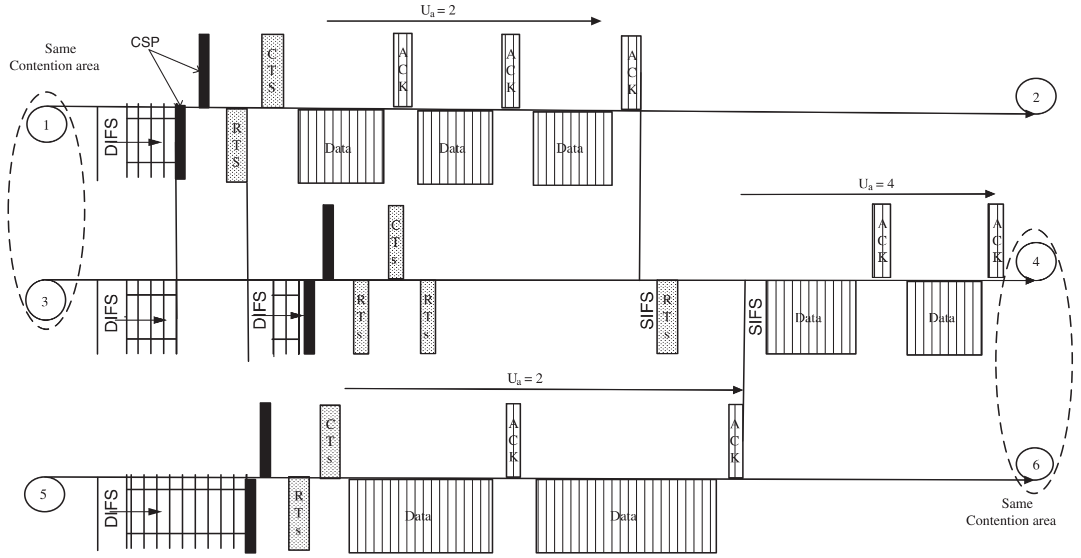


**Figure 4.** The multiple input multiple output-aware rate splitting scheme under hidden node problem. CSP, channel sounding phase; DIFS, distributed coordination function interframe space; SIFS, short interframe space; RTS, ready to send; CTS, clear to send; ACK, acknowledgement.

desirable slot alongside all other alternative valid slots, so that the receiver chooses from them if needed. If an alternative slot is selected, the transmitter broadcasts the new selected slot in another RTS packet so that overhearing nodes can update their reservation tables. To prevent the reserved slot from being violated by other absent connection pairs (connection pairs that did not hear the broadcasted reservation information because they were busy communicating with their pairs), the reserving connection pairs are required to resend a resource reclaiming frame (i.e., RTS) that has the reserved slot's RA. Figure 4 shows how connection pair (3–4) reserves a slot while connection pair (1–2) is busy. In such scenario, connection pair (3–4) resends another RTS frame after short IFS (SIFS) time interval from the end of the transmission of connection pair (1–2). This is required to let connection pair (1–2) know about the reserved slot of the connection pair (3–4).

Because nodes must be able to decode and store the CSI and the broadcasted reserved slot RA in their NAV table, the CSP and SSBP must use a channel coding scheme known to all nodes, although connections can exploit different channel coding schemes for data communications during the reserved slot period.

The SSBP starts after finishing the CSP and collecting the CSI information. To explain the procedure of finding an appropriate slot period and determining its reservation information, we first define the following variables:

- $z_i,\ i = \{1, 2, \ldots, \Psi\}$, is the $z_{i\text{th}}$ connection out of the $\Psi$ connection pairs that have already reserved a slot.
- $\epsilon_s^{z_i}$ is the slot start time of the $z_{i\text{th}}$ connection.
- $\epsilon_e^{z_i}$ is the slot end time of the $z_{i\text{th}}$ connection.
- $U_a^{z_i}$ is the number of antennas intended to be used and broadcasted by the $z_{i\text{th}}$ connection.
- $H_I^{z_i}$ is the CSI of the $z_{i\text{th}}$ interfering connection.
- $I_t^{z_i}$ is the tolerated interference for the $z_{i\text{th}}$ connection.
- $R_{\text{req}}$ is the requested data rate (Mbps) of the upper layers.

To illustrate the SSBP, let us consider that, at the time when the accessing pair starts the algorithm, there exist two reservations: pair A and pair B reservations. Pair A's slot starts from $\xi_s^A$ to $\xi_e^A$ and pair B's starts from $\xi_s^B$ to $\xi_e^B$. Pairs A and B each use two antennas, that is, $U_a^A = 2$ and $U_a^B = 2$, respectively. Figure 5 depicts the reserved slot's starting and ending time and the antennas used on each pair. Algorithm 1 details the procedure that the accessing connection uses in order to find an appropriate slot.

## The MRS algorithm:

Because the ending or starting time of a slot means either releasing or engaging spatial channel(s), we check for spatial channels' condition at the start or the end of any slot period. The operation in line 1 of the MRS Algorithm 1 points according to time in which a slot starts or finishes in ascending order. The algorithm in lines 3–11 differentiates between the start and the end of reserved slots. When it

 *Wirel. Commun. Mob. Comput.* 2014; **14**:339–354 © 2012 John Wiley & Sons, Ltd.
DOI: 10.1002/wcm

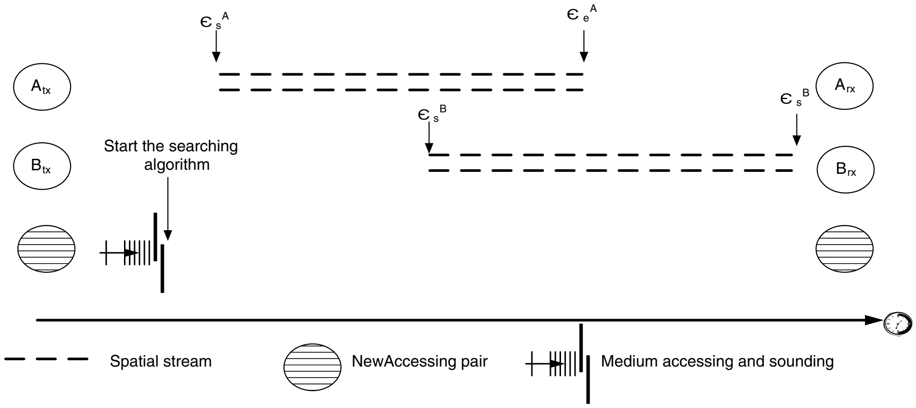


**Figure 5.** Reserved slot(s) information.

**Algorithm 1** Finding an appropriate slot

INPUT:

- $(\epsilon_s^{z_i}, \epsilon_e^{z_i}, U_a^{z_i}, H_I^{z_i}, I_t^{z_i}),\ z_i, i = \{1, 2, \ldots, \Psi\}$
- $H_d$

$A \longleftarrow \{\ldots, \xi_j, \ldots\} \longleftarrow \underset{time}{sort}(\epsilon_s^{z_i}, \epsilon_e^{z_i}), \forall i$
**for** all $\xi_{j^{th}} \in A$ **do**
    **if** $\xi_{j^{th}}$ is a start of transmission **then**
        $H \longleftarrow horzcat[H_d,\ horzcat[H_I,\ H_I^{z_j}]]$
        $U_a \longleftarrow U_a + U_a^{z_j}$
        $I_t \longleftarrow \min(I_t^{z_{j-1}}, I_t^{z_j})$
    **else**
        $H \longleftarrow horzcat(H_d,\ H_I(:,\ H_I^{z_j}))$
        $U_a \longleftarrow U_a - U_a^{z_j}$
        $I_t \longleftarrow I_t + I_t^{z_j}$
    **end if**
    $U_r \longleftarrow (\varphi - U_a)$
    **while** $C_i < R_{req}$ and $\tilde{n}_t \leq U_r$ **do**
        $increment(\tilde{n}_t)$
        $C_i \longleftarrow Equation(5) \longleftarrow (H, \tilde{n}_t)$
    **end while**
    **if** $C_i \geq R_{req}$ **then**
        $I_g \longleftarrow Equation(7) \longleftarrow (H_d, \tilde{n}_t)$
        $S_L \longleftarrow (\xi_{j+1} - \tilde{\xi})$
        **if** $I_g \leq I_t$ **then**
            **if** $S_L^{req} \geq S_L$ **then**
                $clm \longleftarrow size(H)$
                $\tilde{I}_t \longleftarrow Equation(8) \longleftarrow (H, clm, \tilde{n}_t)$
                **return** $(\tilde{\xi}, \tilde{\epsilon_e}, \tilde{n}_t, \tilde{I}_t)$
            **end if**
        **else**
            $\tilde{\xi} \longleftarrow \xi_{j+1}$
        **end if**
    **else**
        $\tilde{\xi} \longleftarrow \xi_{j+1}$
    **end if**
**end for**

| | | | |
|---|---|---|---|
| $H$: | Temporal matrix. | $U_a$: | Antennas used. |
| $I_t$: | Tolerated interference. | $U_r$: | Remained or unused antennas. |
| $S_l$: | Slot length. | $S_L^{req}$: | Requested slot length. |
| $clm$: | Total number of columns of a matrix. | $\tilde{\xi}$: | Valid start time of a TXOP slot. |

is a start of a slot, the algorithm in lines 4–6 concatenate the channel coefficient matrix of this connection to the temporal matrix $H$ and then computes the actively used antennas and tolerated interference in the following two lines, respectively. At the end of a slot, the algorithm in lines 8–10 deconcatenates (removes) the channel coefficient matrix of the finishing slot from the temporal matrix $H$ and then computes the actively used antennas and tolerated interference. The code in line 12 computes the remaining or unused antennas, which are then incrementally used in the while loop, lines 13–16, to estimate the attained channel capacity, $C_i$. Using $H$ and $U_r$, the algorithm in lines 13–16 incrementally increases the number of active antennas (used) and computes the possible achievable rate. If the requested rate is reached by any number of the available resources, the while loop returns the required antennas, $\tilde{n}_t$. If the requested rate is attained as indicated by the code in line 17, the algorithm checks whether the generated interference, by using the required antenna, can be tolerable by other connections. This is carried out by comparing the generated interference, $I_g$, with the tolerated interference, $I_t^{z_i}$, broadcasted by other connections. The generated interference is computed using the interfering matrix of the $z_{i\text{th}}$ connection, $H_I^{z_i}$, and by assuming that the channel fading from transmitter to receiver is similar to that from the receiver to the transmitter. Given the required antennas $\tilde{n}_t$, returned from the while loop, and $H_I^{z_i}$, the accessing node can compute $I_g$ using the equation

$$I_g = \sum_{i=1}^{\tilde{n}_t} \sum_{j=1}^{n_r} h_I(i, j) P_i \tag{7}$$

where $h_I(i, j)$ is the channel fading coefficient from the $j$th transmitting (interfering) antenna of the $z_{i\text{th}}$ connection to this connection. If a valid slot period with the required supported data rate is found (lines 20–26), the accessing pair computes the tolerated interference $\tilde{I}_t$, which should not be exceeded by other connections if concurrent slots are to be scheduled. The tolerated interference is computed using the expression

$$\tilde{I}_t = \sum_{i=\tilde{n}_t}^{Q} \sum_{j=1}^{n_r} h(j, i) P_i \tag{8}$$

where $Q$ is the total number of columns of the $H$ matrix and $h(j, i)$ is the channel fading coefficient at the $j$th row and the $i$th column of the $H$ matrix.[‡] The code in lines 27 and 30 show the case when the current slot interval is not a valid slot. In such case, the algorithm jumps to the next interval, which is represented by the next channel characteristic change point.

In case when there is no previously reserved slot by any connection pair around either the transmitter or the receiver, the accessing pair can schedule their slot to any time to satisfy their quality-of-service requirements. Slot reservation in such case is straightforward. On the basis of the CSI information, nodes first determine the number of required antennas, next the desired start time, and last the slot length during which the connection pair holds the required resources (i.e., antennas).

The execution of the MRS Algorithm 1 results in defining multiple valid slots with their RAs $(\tilde{\xi}, \tilde{\epsilon}, \tilde{n}_t, \tilde{I}_t)$. These valid slots and their RAs are then broadcasted using RTS and CTS exchanges and stored by nodes that overhear them. Multiple valid slots are required in case of slot mismatch, which can be caused by the hidden node problem. Slot mismatch is induced by the fact that the description of these valid slots (i.e., $(\tilde{\xi}, \tilde{\epsilon}, \tilde{n_t}, \tilde{I_t})$) on the transmitter side is different from that on the receiver side. Finally, nodes then use their reserved slots to start data communication. We mention here, in closing, that implementation complexity-wise, the proposed MRS algorithm as described previously may incur higher complexity than the legacy IEEE 802.11n because more decision steps are involved in the algorithm compared with 802.11n. However, the throughput enhancement provided by the proposed algorithm is a reasonable motivation for its deployment.

## 4. MULTIPLE INPUT MULTIPLE OUTPUT-AWARE RATE SPLITTING SCHEME PROPERTIES

In this section, we introduce some properties of the MRS MAC protocol that reveals other advantages of the MRS protocol.

- ***Property 1***: When scheduling multiple connection pairs with interfering distance $R$ greater than their communication distance $D$, the system capacity increases as the ratio $D/R$ decreases.

  *Proof*. Referring to the system model explained in Section 2, we have $k$ connection pairs. Receivers of these connections receive a desirable signal from their desirable transmitters and $\Gamma$ interfering signals from interfering transmitters. Let $R_i, i = \{1, 2, \ldots, \Gamma\}$, represent the distance between this connection pair and the $\Gamma$th interfering connection pairs. Let $\tilde{n}_t$ and $\tilde{n}_r$ represent the active transmit and receive antennas at each connection pair, that is, the transmitter and receiver, respectively. Let $C_T$ denote the total achievable system capacity and is given by

‡We should clarify here that the expressions for $I_g$ and $\tilde{I}_t$ assume flat-fading models for the user channel statistics. Thus, the behavior of the MRS algorithm in mobile environments or variable topologies are not investigated in this paper.

$$C_{\mathrm{T}} = \sum_{j=\vartheta=1}^{k} \sum_{i=1}^{\tilde{n}_{\mathrm{t}}} \log_2 \left( \frac{1 + P_j h_i^H h_i}{I_{\tilde{n}_{\mathrm{r}}} + \mathrm{horzcat}\left[ P_j \tilde{H}_\vartheta \tilde{H}_\vartheta^H \quad \mathrm{horzcat}\left[ P_j H_j H_j^H \right]_{\forall\, j: j \neq \vartheta} \right]} \right) \quad (9)$$

where $P_j$ is the transmission power of the $j$th transmit antenna element at the $v_{j\mathrm{th}}^{\mathrm{tx}}$ transmitting node, $h_i$ is the $i$th column of the channel coefficients matrix of the desired transmitter, $H_\vartheta$, $\tilde{H}_\vartheta$ is the remaining matrix after removing the $i$th column out of $H_\vartheta$, $H_j$ is the channel fading coefficients matrix of $j$th interfering node, $I_{\tilde{n}_{\mathrm{r}}}$ is the $(\tilde{n}_{\mathrm{t}} \times \tilde{n}_{\mathrm{r}})$ identity matrix.

For simplicity, we assume that the transmission power of all transmitting antennas is the same. The channel coefficient matrix estimated by $v_{i\mathrm{th}}^{\mathrm{rx}}$ receiver can be represented as

$$H_j = \begin{bmatrix} h_j(1,1) & \dots & h_j(1,\tilde{n}_{\mathrm{t}}) \\ \vdots & \ddots & \vdots \\ h_j(\tilde{n}_{\mathrm{r}},1) & \dots & h_j(\tilde{n}_{\mathrm{r}},\tilde{n}_{\mathrm{t}}) \end{bmatrix}, j = 1, \dots, k \quad (10)$$

where $h_j(\tilde{n}_{\mathrm{r}}, \tilde{n}_{\mathrm{t}})$ is the channel fading coefficient between the $i$th receive element of this node to the $j$th transmit element of the $v_{j\mathrm{th}}^{\mathrm{tx}}$ transmit node and is given by

$$h_j(\tilde{n}_{\mathrm{r}}, \tilde{n}_{\mathrm{t}}) = \begin{cases} (\frac{\lambda}{4\pi D})^\eta + \chi_\sigma & \text{if } j = \gamma \\ (\frac{\lambda}{4\pi R})^\eta + \chi_\sigma & \text{if } j \neq \gamma \end{cases} \quad (11)$$

Equation (9) can be rewritten as

$$C_{\mathrm{T}} = \sum_{j=1}^{k} \sum_{i=1}^{\tilde{n}_{\mathrm{t}}} \log_2 \left( \frac{1 + P_j h_i^H h_i}{I_{\tilde{n}_{\mathrm{r}}} + P_j H_j H_j^H} \right) \quad (12)$$

Hence, by fixing $D$ and assigning larger values for $R$, the channel fading coefficient factor, $h_j(\tilde{n}_{\mathrm{r}}, \tilde{n}_{\mathrm{t}})$, of the interfering connections further decrease, which increases the signal-to-interference-plus-noise ratio per connection pair. From Equation (12), having a higher signal-to-interference-plus-noise ratio per connection can collectively produce higher system usability. Thus, the system capacity increases as the ratio $D/R$ decreases.

***Advantages***: This property can be utilized to maximize the system usability by scheduling multiple concurrent connections with the least interference on one another.

- ***Property 2***: The MRS MAC protocol can converge to the IEEE 802.11 MAC protocol by switching off the CSP.
  *Proof*. To translate the required rate into numbers of antenna requirements, the MRS MAC protocol extends the IEEE 802.11 MAC protocol by considering the CSP, which is then used to compute the required antennas. By switching off the CSP and requesting all antennas, the MRS MAC protocol completely converges to the IEEE 802.11 MAC protocol.
  ***Advantages***: This property is very beneficial in systems where legacy IEEE 802.11n stations exist, and it is desirable to utilize the concurrent bandwidth partitioning mechanism with MRS capable stations. For example, in wireless mesh networks, the mesh access point stations are required to communicate with peer mesh points and users. Hence, the mesh access point can exploit the concurrent bandwidth sharing protocol with peer mesh points and switch to the IEEE 802.11 MAC to communicate with legacy users.
- ***Property 3***: The MRS MAC protocol permits an independent channel coding and decoding mechanism of individual pairs of nodes during their reserved slot.
  ***Discussion***: Because connection pairs and nodes around them are not required to exchange any coordination information during the data CP, the MRS MAC protocol permits connection pairs to implement their own desirable channel coding and decoding schemes during their reserved slot periods.
  ***Advantages***: Such property allows connection pairs during the CP to use any channel coding structure and decoding scheme that suits their instantaneous channel status. This results in improving the channel quality of different connection pairs based on their instantaneous channel status. Also, connection pairs and nodes around them know the channel fading characteristics of each other. Hence, they can consider the received signal from other pairs as an interference signal, and they can apply any interference cancellation technique.
- ***Property 4***: With MRS MAC protocol, connection pairs can optionally schedule their slot at any desired time.
  ***Discussion***: Given the searching procedure for valid slots as explained by Algorithm 1, the MRS MAC protocol stipulates the following means for protecting the reserved slot:
  (1) Contending nodes pause when they hear the start of SFs exchange as depicted in Figures 3–4. This allows nodes to update their NAV table for all reserved slots of other connection pairs.
  (2) Successful four-way handshakes (channel sounding and RTS–CTS frame exchange) further guarantee the slot reservations. Nodes that miss receiving the SFs because of collision are likely to receive the reservation

frame exchanges. In addition, transmitting the sounding and RTS–CTS frames over multiple delayed intervals can further assure the reception of the CSP and/or SSBP frame exchanges.

(3) Connection pairs are only allowed to reserve a slot if their used resources do not violate the constraints broadcasted by other connection pairs for that slot. These constraints include not exceeding the upper limit of the used spatial streams and the tolerated interference of other connections during that slot.

(4) Reservation information of all reserved slots are rebroadcasted by any new reservation that follows.

(5) The MRS protocol prioritizes the reserved slot by allowing connections to use SIFS to access the transmission medium prior to their reserved slot.

(6) To prevent the reserved slots from being violated by other absent connection pairs, the reserving connection pair resends a resource reclaiming frame that have the slot reservation information. Figure 6 depicts how connection pair $P_2$, which reserved a slot while pair $P_1$ is busy communicating, sends a reclaiming frame after $P_1$'s end of transmission to let the latter pair know about the reserved slot.

(7) Connection pairs can time out after DIFS time if the allocated bandwidth is not being used yet. Figure 6 also illustrates how pair $P_3$ times out and starts medium access after DIFS time on $P_2$ as the latter did not start CP at the slot start time.

***Advantages***:

– Providing delay differentiation: Flexibility of scheduling flows with more stringent delay bound allows more flows to meet their delay constraints.
– Maximizing system usability: Concurrently scheduling connection pairs that have less interference effect on one another can increase the achievable data rate of each pair and hence increase the overall system capacity.
– Maximizing bandwidth utilization: All the remaining antennas are used during all intervals.

- ***Property 5***: By scheduling appropriate slots to access classes on the basis of their delay bound and system resources, the MRS MAC protocol can provide delay differentiation.

***Discussion***: Let $FL = \{fl_i : \quad i = 1, 2, \ldots, \sigma\}$ represent a set of access classes for which a slot is scheduled. Without loss of generality, assume the quality-of-service requirements of an access class, $fl_i$, are described by

  ○ $r_{\mathrm{r}}^{i}$: the requested bandwidth (bps).
  ○ $d_b$: the delay bound.

Let $S = \{s_i : \quad i = 1, 2, \ldots, \delta\}$ represent the set of slots. Each slot, $s_i$, is described by following tuples:

  ○ $r_{\mathrm{a}}^{i}$: the available rate.
  ○ $\epsilon_{\mathrm{s}}^{i}$: the slot start time.
  ○ $\epsilon_{\mathrm{e}}^{i}$: the slot end time.

Algorithm 2 allocates the appropriate slot to access classes according to the weight of their maximum tolerated delay bound and channel utilization. Scheduling access classes close to their delay bound can save slots for access classes with a more stringent delay

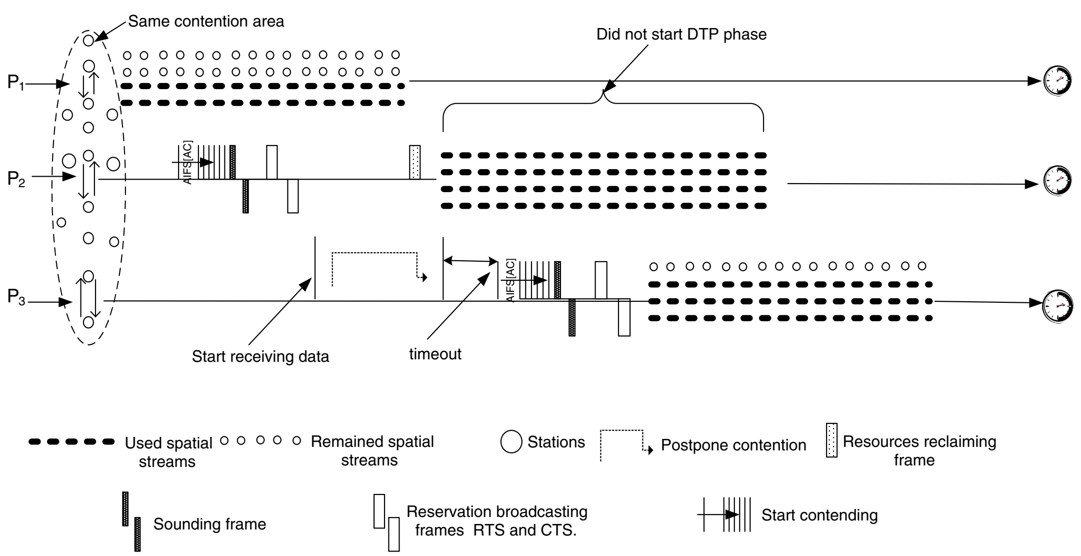


**Figure 6.** Some functional aspects of the multiple input multiple output-aware rate splitting medium access control protocol. RTS, ready to send; CTS, clear to send; AIFS[AC], arbitration interframe space [access class] ; DTP, distributed transmission protocol.


*Wirel. Commun. Mob. Comput.* 2014; **14**:339–354 © 2012 John Wiley & Sons, Ltd.
DOI: 10.1002/wcm

**Algorithm 2** Time slots to most delay constraints

INPUT:
- FL: set of flows
- S: set of slots

1: **for** all $f_i \in FL$ **do**
2: $\quad d_b \longleftarrow f_i$
3: $\quad r_r \longleftarrow f_i$
4: $\quad$ **for** all $s_i \in S$ **do**
5: $\qquad \epsilon_e^i \longleftarrow s_i$
6: $\qquad r_a^i \longleftarrow s_i$
7: $\qquad O_i \longleftarrow \dfrac{\epsilon_e^i}{d_b} + \dfrac{r_r}{r_a^i}$
8: $\quad$ **end for**
9: $\quad$ **return** $\max(o_i)$
10: **end for**

bound. Coupling the previous allocation criteria with maximizing bandwidth utilization can further optimize the bandwidth to serve more access classes. Algorithm 2 describes the procedure of finding the most tolerable slot in terms of delay constraint.

For each access class, the algorithm first stores the delay bound and requested rate as shown by the code in lines 2 and 3. For each available slot, we store the start time and the available rate as described by the algorithm in lines 5 and 6. Given the stored information, that is, the slot start time, delay bound, requested rate, and the available rate, the algorithm in line 7 computes the tolerable ratio of the $i$th slot. Lastly, the algorithm (line 9) returns the maximum tolerable ratio of all slots $o_i$.

## 5. PERFORMANCE EVALUATION

In this section, we evaluate the performance of the MRS protocol. We first detail the simulation model and then present simulation results. The results are compared with the IEEE 802.11n protocol.

### 5.1. Simulation model

Utilizing the OPNET modules, we modified the inbuilt IEEE 802.11 physical and MAC layers in the OPNET Modeler of MRS MAC protocol as explained previously. These modifications include the following:

- Multiple transmit and receive antenna elements were added. Each transmit and receive antenna element is modeled using the built-in wireless transmit and receive module of the OPNET Modeler, respectively. Similar to the IEEE 802.11n draft [12], we considered that $n_t = n_r = 4$. We also modified the legacy model to perform spatial stream multiplexing and demultiplexing.
- The interaction between the physical and MAC layers to accommodate the increased number of transmit and receive antenna elements were modified.
- The SF transmission phase, which includes exchanging the SFs through all transmit and receive antenna elements of the transmitter and its intended receiver, was inserted.
- The packet structure of the SF using the Packet Module of OPNET was built.
- Upon receiving the SFs transmitted, receive antenna models estimate the channel fading coefficient $h_d(i, j)$ of all the received SFs. The results are then used to construct the channel sounding matrix $H_d$. Similarly, the overhearing receivers in the same coverage area use the received SFs to estimate the channel fading coefficient and to construct the $H_I^i$.
- The NAV table of the IEEE 802.11 model to maintain the updated number of remaining and used antennas (spatial streams) was modified.
- To estimate the achieved channel capacity under different interference zones, we interfaced the OPNET Modeler with MATLAB simulation tools. The OPNET Modeler is used to model the MAC layer, whereas MATLAB is used to model the physical layer. The MAC layer sends $H_d$, $H_I^i$, $D$, $R$, and $\tilde{n_t}$ to the MATLAB. The latter then computes the achieved capacity and returns the result.
- The instantaneous medium status (i.e., busy, idle, or collision) was also modified according to Equation (6). The modification includes modifying the state transition diagram of the original model and the interaction between the physical and MAC layers. Figure 7 models the instantaneous signal decode ability model that we used in our model. To explain this figure, we consider a receiver equipped with four receiving antennas and five transmitting nodes, each equipped with one transmitting antenna. We consider that the receiver can receive and decode all the incoming spatial streams as long as the number of spatial streams is fewer or equal to the number of receiving

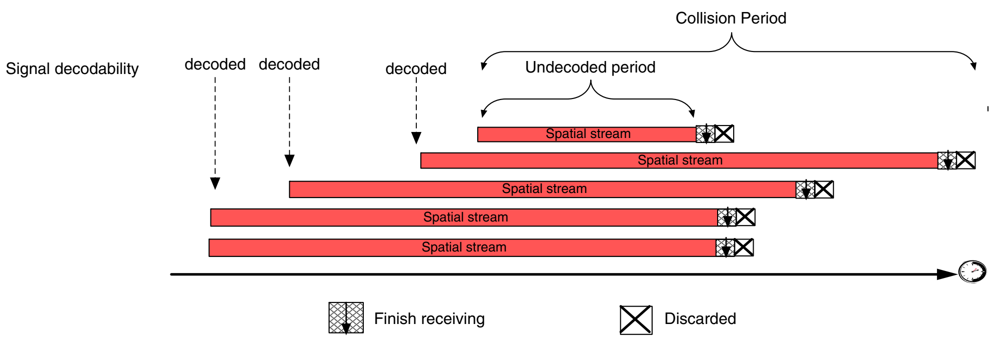


**Figure 7.** Instantaneous signal decode-ability with $\varphi = 4$.

antennas $n_r$. If these transmitters start transmitting their streams, the instantaneous signal decode ability at the receiver is modeled as shown in Figure 7. Spatial streams that experience any collision period are discarded at the end. We also consider that if a collision occurs, the collision period lasts as long as the received signal has an overlapping portion with the collided signals.

- Because IEEE 802.11n is not yet included in the OPNET Modeler, we have also modified the IEEE 802.11 module to include the defined IEEE 802.11n physical and MAC enhancements. This includes adding multiple transmit and receive antennas that are attached to the multiplexing and demultiplexing module.
- The values of the physical and MAC layers' characteristics used for both models follow those defined for the IEEE 802.11n amendment, which are summarized in Table I.

Nodes are configured to generate traffic according to Poisson distribution with mean arrival equal to $\lambda$. The latter is a simulation parameter that assumes different values to model the network loads. For each generated data packet, the nodes select a random neighbor as the final destination for this packet. The transmission rate (Mbps), with no interference at $D = 250$ m is computed and used for MIMO-aware modified IEEE 802.11 and MRS protocol. The former schedules the entire supported data rate,

**Table I.** IEEE 802.11n parameter settings.

| Parameter | Value |
|---|---|
| $CW_{min}$ | 15 |
| $CW_{max}$ | 1023 |
| SIFS | 16 µs |
| PMDU | 500–65,535 bytes |
| RIFS | 2 µs |
| $q$ | 30 µs |

SIFS, short interframe space; PMDU, phase modulation diversity unit; RIFS, reduced interframe space.

whereas the MRS protocol shares the supported data rate via utilizing the multiple spatial channels created by multiple antennas system. During the simulation, we change the following parameters:

- Desired distance ($D$): the communication distance (m) between the transmitter and its intended receiver.
- Interference distance ($R$): the distance (m) between the receiver and the transmitter of the received interfering signal.
- Requested rate ($R_{req}$) window: window of request rates from which a desirable requested rate is selected using uniform distribution function.

### 5.2. Performance metrics

We observe the following performance metrics:

- Average throughput: the total number of successfully delivered bits divided by the lifetime of the simulation.
- Average medium access delay: the average time from inserting the packet in the queue until it starts transmission.
- Achieved rate: the instantaneous supported physical data rate (Mbps) computed before transmission.

### 5.3. Simulation results

To examine the effects of the interference on the system throughput, we consider the scenario in Figure 8(a) where we vary two parameters $D$ and $R$ for the two connection pairs $P_1$ and $P_2$. For this scenario, no MAC protocol is used. Each transmitter generates data for its intended connection pair receiver. Before transmission, the transmitter first exchanges the SFs to get the CSI information, $H_d$, which is then concatenated with the interference part $H_I^{P_{i\text{th}}}$ of the other interfering connection. The result is then used to compute the total channel capacity using Equation (5), which is then used as the data transmission rate.

The results in Figure 9 show the system throughput at different values of $D$ and $R$, which clearly shows that

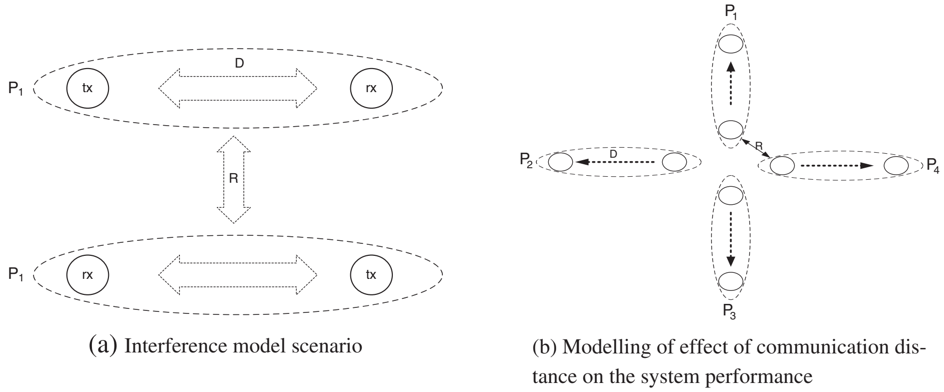


**Figure 8.** The performance scenarios of the multiple input multiple output-aware rate splitting scheme: (a) interference model scenario and (b) modeling of effect of communication distance on the system performance.

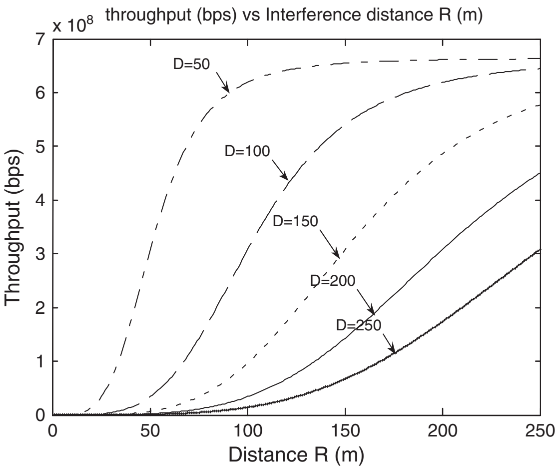


**Figure 9.** Achievable throughput as a function of the communication and interference distance.

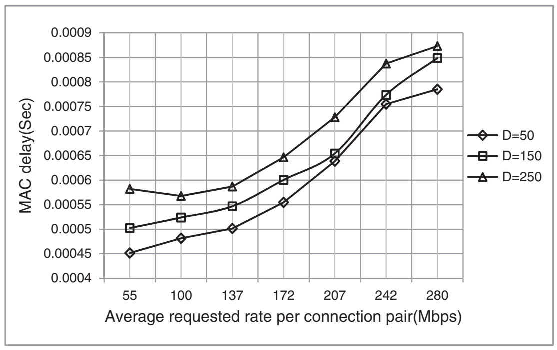


**Figure 10.** Medium access delay for different ranges.

larger values of $R$ reduce the interference effect and hence allow the other connection pair to achieve a higher data rate. Note that connections communicating over a smaller distance $D$ are less affected by the interference. The performance of the MRS protocol is compared with the MIMO-aware modified IEEE 802.11 MAC protocol. To evaluate the performance of the MRS protocol under different values of $D$, $R$, and $k$, we place four connection pairs, that is, $P_1$, $P_2$, $P_3$, and $P_4$, in a circle, as shown in Figure 8(b), with equal interference distance $R$ from each other so that the effects of interference remain fixed during the simulation. For each simulation run, we vary $D$ and hence the requested rate $R_{req}$, where the former is assigned to one of the following: 50, 100, and 150 m. On the other hand, the latter is randomly selected from different ranges: 50-85, 85–120, 120–155, 155–190, 190–260, and 260–300 Mbps. During each simulation run, one range is considered and one value is selected as the requested rate using the uniform distribution function from the selected range. Figure 10 relates the requested rates to the medium access delay. Increasing the amount of the requested rate apparently increases the experienced MAC delay. Larger communication distances $D$ cause higher channel attenuation, which proportionally requires more antennas (spatial channels) to attain the same requested rate. On the other hand, communicating over smaller distances $D$ leads to higher proportional supported data rate per spatial channel, hence requesting a higher data rate, as connections with shorter communication distance $D$ tend to have better performance compared with satisfying the same requested rate at a larger communication distance. Higher sharing of the spatial channels for small requested data rates produce higher throughput (Figure 11).

To further examine the effects of the communication distance $D$ on the system performance, we fix the interference distance $R$ and the requested rate $R_{req}$ at each simulation run. For each simulation run, $R_{req}$ is assigned a value from 50, 200, or 300 Mbps. $R$ is fixed at approximately 180 m. $D$, at each simulation run, is set to one of the following: 50, 100, 150, 200, or 250 m. Results in Figure 12 and 13 clearly show that a larger value of $D$ results in increased delay and lower throughput.

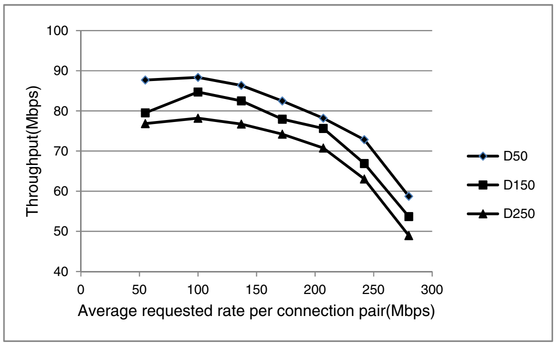


**Figure 11.** Throughput for different ranges of requested rates.

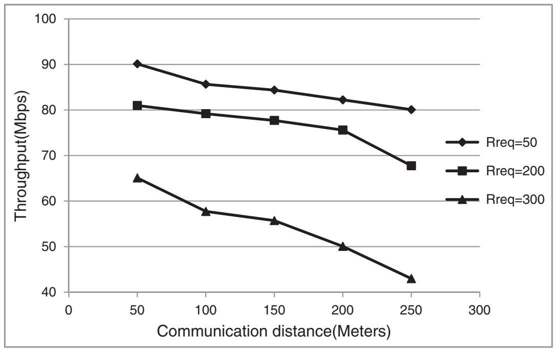


**Figure 13.** Throughput for different values of *D*.

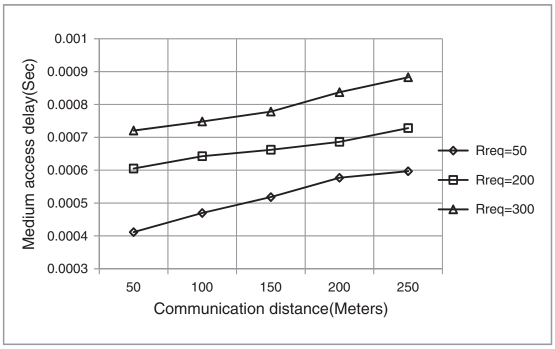


**Figure 12.** Medium access delay for different values of *D*.

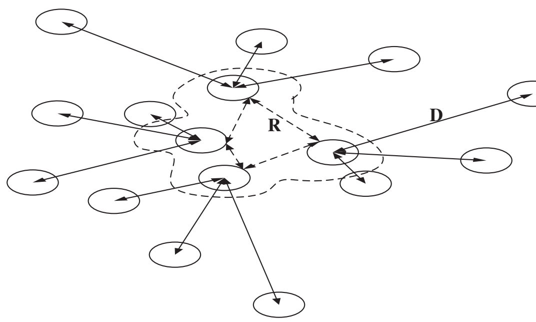


**Figure 14.** Wireless mesh network model.

To compare the performance of the MRS scheme with the MIMO-aware modified IEEE 802.11 MAC protocol, a generalized ad hoc network topology is considered, as shown in Figure 14. Different settings are obtained by varying *D* and *R* such that their average distance remains the same for all the 10 topology settings used. The IEEE 802.11 MIMO-aware MAC protocol uses the entire achievable capacity, whereas the MRS MAC protocol uses $R_{req}$ that is uniformly selected from the range 50–300 Mbps.

Results in Figure 15(a,b) depict the average medium access delay and achievable throughput over 10 simulated cases, with average values of *D* and *R* at 150 and 100 m, respectively.

To further demonstrate the effectiveness of the MRS MAC protocol, we show in Figure 16 the transient

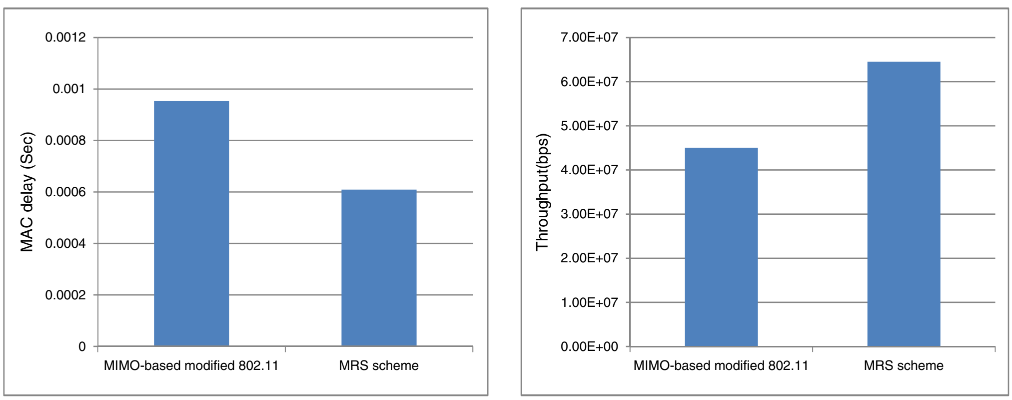


(a) Medium access delay difference (b) The throughput difference

**Figure 15.** Performance comparison between the IEEE 802.11 and multiple input multiple output-aware rate splitting medium access control protocol: (a) medium access delay difference and (b) the throughput difference.


*Wirel. Commun. Mob. Comput.* 2014; **14**:339–354 © 2012 John Wiley & Sons, Ltd.
DOI: 10.1002/wcm

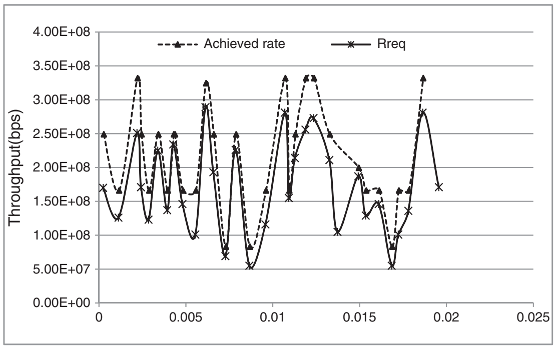


**Figure 16.** Comparison of requested and achieved rates.

performance of the protocol over an interval of 0.02 s for a tagged node in the experiment previously. The results show that the requested rate can always be attained throughout the simulation run.

## 6. CONCLUSION

In this paper, we introduced a novel MRS MAC protocol. Instead of allocating the maximum bandwidth achieved by MIMO communication systems, as defined in the IEEE 802.11n, MRS introduces an efficient concurrent bandwidth sharing scheme that is based on sharing the spatial channels. We detailed the MRS's phases, which include, medium contention control, which is conditioned on the number of used spatial stream; CSP used for exchanging small frames over all antennas, between the transmitter and its intended receiver, to assess the channel between them; SSBP procedure, which uses the CSI obtained from the channel estimation phase to find the appropriate slot period with the desired bandwidth (antennas) and to transmit its reservation attributes using RTS–CTS exchange; and lastly, the CP during which the connection pair start and end their data and ACK packet exchanges. The possibility of efficiently sharing the spatial streams of MIMO systems enabled by MRS scheme opens new research direction for many bandwidth management schemes to maximize the system usability. The performance of MRS is evaluated under different scenarios for different rate demands, interference scenarios, and communication environments. The results were compared with those of the MIMO-aware modified IEEE 802.11 MAC protocol. Results showed that our proposed MRS scheme outperforms the IEEE 802.11n modified model in medium access delay and throughput. We also showed that nodes can always attain their requested rate using the purposed MRS scheme.

## ACKNOWLEDGEMENT

This work is supported by a grant (No. 09-ELE928-02) from The National Plan for Science and Technology (NPST), King Saud University, Saudi Arabia.

## REFERENCES

1. Paulraj A, Nabar R, Gore D. *Introduction to Space-Time Wireless Communication*. Cambridge University Press: United Kingdom, 2003.
2. Gesbert D, Shafi M, Da-shan S, Smith PJ, Naguib A. From theory to practice: an overview of MIMO space-time coded wireless systems. *IEEE Journal on Selected Areas in Communications* 2003; **21**(3): 281–302.
3. Sundaresan K, Sivakumar R, Ingram MA, Chang T. Medium access control in ad hoc networks with MIMO links: optimization considerations and algorithms. *IEEE Transactions on Mobile Computing* 2004; **3**(4): 350–365.
4. Minyoung P, Heath RW, Nettles SM. Improving throughput and fairness for MIMO ad hoc networks using antenna selection diversity, In *IEEE Global Telecommunications Conference*, Austin, TX, USA, 2004; 3363–3367.
5. Mirkovic J, Orfanos G, Reumerman H-J, Denteneer D. A MAC protocol for MIMO based IEEE 802.11 wireless local area networks, In *IEEE Wireless Communications and Networking Conference*, Hongkong, China, 2007; 2131–2136.
6. Redi J, Watson B, Ramanathan R, Basu P. Design and implementation of a MIMO MAC protocol for ad hoc networking. *IEEE Wireless Sensing and Processing* 2006; **6248**: 231–238.
7. Kulkarni G, Nandan A, Gerla M, Srivastava M. MIMAC: a rate adaptive MAC protocol for MIMO-based wireless networks, In *UCLA CSD*, 2004; 535–542.
8. Dechene J, Meerja KA, Shami A, Primak S. A novel MIMO-aware distributed media access control scheme for IEEE 802.11 wireless local area networks, In *IEEE Conference on Local Computer Networks*, Dublin, Ireland, 2007; 125–132.
9. Mundarath JC, Ramanathan P, Van Veen BD. NULL-HOC : a MAC protocol for adaptive antenna array based wireless ad hoc networks in multipath environments, In *IEEE Global Telecommunications Conference*, Dallas, TX, USA, 2004; 2765–2769.
10. Joon-Sang P, Nandan A, Gerla M, Heechoon L. SPACE-MAC: enabling spatial reuse using MIMO channel-aware MAC, In *IEEE International Conference on Communications*, Seoul, Korea, 2005; 3642–3646.
11. Ashtaiwi A, Hassanein H. MIMO-based collision avoidance in IEEE 802.11e networks. *IEEE Transactions on Vehicular Technology* 2010; **59**(3): 1076–1086.
12. IEEE P802.11n–D4.0. Wireless LAN Medium Access Control (MAC) and Physical Layer (PHY)

specifications: Enhancements for Higher Throughput. *IEEE Draft* 2008.
13. Jafar SA, Fakhereddin MJ. Degrees of freedom for the MIMO interference channel. *IEEE Transaction on Information Theory* 2007; **53**(7): 962–968.
14. Tse D, Viswanath P. *Fundamentals of Wireless Communication*. Cambridge University Press: United Kingdom, 2005.
15. MathWorks. www.mathworks.com [Accessed on 2010].

## AUTHORS' BIOGRAPHIES

**Abduladhim Ashtaiwi** (A'09) received his B.Sc. degree in Electrical and Electronic Engineering from Bright Star University of Technology, Brega Hereby, Libya, in 1992 and his M.Sc. and Ph.D. degrees from Queen's University, Kingston, ON, Canada, in 2004 and 2009, respectively.

He was a research associate in the Department of Electrical and Computer Engineering, Queen's University, in 2009. He has authored several publications, including journal papers, refereed conference proceeding papers, and book chapters. His research interests include fourth-generation-and-beyond wireless network architectures, wireless local area network protocols and standards, cross-layer design and optimization, multiple-input-multiple-output systems, wireless ad hoc and sensor networks, radio resource management, wireless medium access control techniques, quality-of-service routing, and resource reservation.

**Ahmed Iyanda Sulyman** (M'04-SM'09) was born in 1968. He obtained his PhD degree in Electrical Engineering from Queen's University, Canada, in 2006. He was a Teaching Fellow at the Department of Electrical Engineering, Queen's University, in 2004-2006; a Post-Doctoral Research Fellow at the School of Computing Queen's University, in 2007 and at the Royal Military College of Canada, in 2008-2009. Since February 2009, he has been with the Department of Electrical Engineering at King Saud University, Riyadh, Saudi Arabia, where he is currently working as an assistant professor. He is a senior member of the IEEE and has served as co-chair in IEEE conferences and workshops. His research interest is in wireless communications and networks.

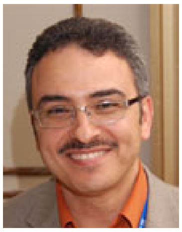

**Hossam S. Hassanein** is with the School of Computing at Queen's University, working in the areas of broadband, wireless, and variable topology networks architecture, protocols, control, and performance evaluation. Hassanein obtained his Ph.D. in Computing Science from the University of Alberta in 1990. He is the founder and director of the Telecommunication Research (TR) Lab (http://www.cs.queensu.ca/∼trl) in the School of Computing at Queen's. Hassanein has more than 350 publications in reputable journals, conferences, and workshops in the areas of computer networks and performance evaluation. He has delivered several plenary talks and tutorials at key international venues, including Unconventional Computing 2007, IEEE ICC 2008, IEEE CCNC 2009, IEEE GCC 2009, IEEE GIIS 2009, ACM MSWIM 2009, and IEEE Globecom 2009. Hassanein has organized and served on the program committee of numerous international conferences and workshops. He also serves on the editorial board of a number of international journals. He is a senior member of the IEEE, and is currently chair of the IEEE Communication Society Technical Committee on Ad hoc and Sensor Networks (TC AHSN). Hassanein is the recipient of Communications and Information Technology Ontario (CITO) Champions of Innovation Research award in 2003. He received several best paper awards, including at IEEE Wireless Communications and Network (2007), IEEE Global Communication Conference (2007), IEEE International Symposium on Computers and Communications (2009), IEEE Local Computer Networks Conference (2009), and ACM Wireless Communication and Mobile Computing (2010). Hassanein is an IEEE Communications Society Distinguished Lecturer.


*Wirel. Commun. Mob. Comput.* 2014; **14**:339–354 © 2012 John Wiley & Sons, Ltd.
DOI: 10.1002/wcm